

# Surface-suppressed electron resonance spectroscopies<sup>a)</sup>

P. Glenn Barkley,<sup>b)</sup> Joseph P. Hornak,<sup>c)</sup> and Jack H. Freed<sup>d)</sup>  
Baker Laboratory of Chemistry, Cornell University, Ithaca, New York 14853

(Received 28 January 1985; accepted 15 October 1985)

Surface-suppressed electron resonance spectroscopies (SSERS) refers to the phenomenon in which stable paramagnetic radicals adsorbed on clean (noble) metal surfaces have their ESR signal suppressed. This phenomenon is studied in some detail by ultra-high-vacuum ESR (UHV-ESR) and cyclotron resonance from microwave-induced secondary electron emissions (CREMSEE) in combination with conventional thermal desorption. The UHV-ESR is performed *in situ* on the inner surface of the microwave cavity after leaking in stable nitroxides as previously described by Nilges and Freed. In the SSERS phenomenon, the first layers of nitroxide deposited on the metal surface do not give rise to an observable ESR signal, even though a significant decrease in the CREMSEE microwave power threshold,  $P_t$ , is observed. It is consistently found (for several nitroxides and noble metals) that an ESR signal is observed only when  $P_t$  has dropped to the order of 20 ( $\pm 10$ )% of its initial value. The ESR signal then increases monotonically with increased dosage. Also, a correlation between these measured reductions in  $P_t$  and the estimated surface coverages required for initial observation of the ESR signal, is suggested by our results. It may be that SSERS is (partly) due to the first layer of nitroxide interacting strongly by exchange forces to the surface conduction band of the metal, so that the ESR signal is too broadened to be observed. Subsequent nitroxide layers may also be affected through their interaction with previous layers by weaker exchange forces. This is consistent with experiments in which a related but diamagnetic species is utilized to form the initial adsorbed layers, and it is found to act as an "insulator" for the subsequent nitroxide layers. (On the other hand, surfaces pretreated with  $O_2$  or  $O_2/H_2O$  mixtures had very little effect on SSERS observed with Ag surfaces, although it had some effect, in the sense of a weak insulator, with Cu surfaces.) The change in ESR signal upon warming was correlated with the observed pressure changes. In some cases there are unusual nonmonotonic variations of the ESR signal strength, inconsistent with observed desorption of nitroxide, that are also believed to be due to SSERS. The possible role of temperature-dependent surface wetting effects is briefly considered.

## I. INTRODUCTION

A question in the field of surface science for which ESR seems eminently suited is the nature of the interaction of paramagnetic molecules with metal surfaces. The possibility to explore this subject stems from recent developments in ultra-high vacuum (UHV) techniques applied to ESR.<sup>1-5</sup> In the UHV-ESR technique, clean metal films may be prepared inside the resonant microwave cavity, and then various gases or molecules with enough vapor pressure ( $\approx 1$  Torr at room temperature) may be allowed to adsorb on these surfaces. ESR is then available to detect surface paramagnetism. Even in the absence of any paramagnetism, the technique of CREMSEE (cyclotron resonance from microwave-induced secondary electron emission) may be used as a sensitive indicator of surface bonding.<sup>2,3</sup> Furthermore, the cleanliness of the evaporated metal film surface can be checked by measuring the work function and comparing with published values. One may measure the work function *in situ* in the microwave

cavity via a modification of the CREMSEE technique: photo-CREMSEE.<sup>4</sup>

In a previous preliminary study we reported on the adsorption of a stable nitroxide free radical DTBN (di-tert-butyl-nitroxide) on noble metal surfaces.<sup>3</sup> Experiments were first performed on a Cu surface that had been extensively air oxidized. Air oxidation leads to an order-of-magnitude drop in the CREMSEE threshold,  $P_t$ , from that for clean Cu. It was possible to observe a dilute rigid-limit ESR spectrum of DTBN on this air-oxidized surface after leaking DTBN into the system and pumping out the physisorbed layer which had yielded a single exchange narrowed ESR line. However, when similar experiments were performed with DTBN on a clean Cu surface, no ESR signals were observed. Yet the observation of a dramatic drop in CREMSEE threshold, when the DTBN was being leaked in, clearly demonstrated that the DTBN is adsorbing on the Cu and forming a strong enough chemical bond to affect secondary electron emission. Bakeout of the cavity at 150 °C returned the CREMSEE threshold to almost its initial value for clean Cu, implying that the DTBN had been effectively desorbed.

This phenomenon, wherein no ESR signal is observed, but the CREMSEE threshold is decreased, we refer to as: surface-suppressed electron resonance spectroscopies (SSERS).

In this work, we report our results on a more extensive

<sup>a)</sup> Supported by the Cornell Materials Science Center (NSF), and by Grant No. DE-AC02-80ER04991 from the Office of Basic Energy Sciences of DOE.

<sup>b)</sup> Present address: Pall Corp., Cortland, New York 13045.

<sup>c)</sup> Present address: Department of Chemistry, Rochester Institute of Technology, Rochester, New York 14623.

<sup>d)</sup> Guggenheim Fellow 1984-1985 (on leave at the École Normale Supérieure, Paris).

study of SSERS. First of all we confirm the original observation of SSERS. But mainly we address the questions of (1) whether it is possible to obtain any ESR signal from a nitroxide on a clean metal surface or must it first be covered; (2) what differences exist between different metals and different nitroxides; (3) what is the role, if any, of surface oxidation vs surface insulation; (4) to what extent can CREMSEE measurements be correlated with a lack of ESR signals. One weakness of our previous study<sup>3</sup> was due to the fact that apparently large, but actually insufficient dosages of nitroxide were typically applied and no systematic (but only a preliminary) study of temperature dependence was made. Thus, for example, those preliminary results suggested that for Ag at low  $T$  ( $\sim -100^\circ\text{C}$ ) there is a signal from a fractional coverage, but Cu requires a very large dosage. Our present results clarify such matters. They show that *in all cases* clean noble metal surfaces exhibit substantial SSERS. Furthermore, once the ESR signal appears above a threshold level of dosage, it increases monotonically with further dosage, usually leveling off to a linear dependence on the dosage. Thus there is no reason whatsoever to suppose that the nitroxide ESR signal observed at low  $T$  is due to adsorption at remaining binding sites on the metal as we previously suggested.

The experiments reported herein are more systematic in that they involve simultaneous CREMSEE and ESR detection during the course of extensive dosage at a constant (low) temperature. Temperature-dependent effects after this dosage are then simultaneously studied by both ESR and by thermal desorption methods as the temperature is gradually raised. What emerges from these studies is a consistent picture: Stable radicals adsorbed on clean noble metal surfaces have their ESR signal suppressed until the adsorbed layers of molecules effectively insulate subsequent layers from the metal surface. The number of layers required depends upon the nitroxide, the metal, and its pretreatment, and it also shows unusual temperature-dependent anomalies. We suggest a model based upon transmission of the effects of the surface conduction band of the metal by the spin exchange between adjacent layers of nitroxide radicals, that acts to so broaden out the ESR signal as to be unobservable.

In Sec. II we describe our experimental methods. Our experimental results on SSERS are described in Sec. III and discussed in Sec. IV. A conclusion appears in Sec. V.

## II. EXPERIMENTAL METHODS

### A. Ultra-high vacuum system

Our newer UHV-ESR system is similar to that illustrated in Ref. 2. Details of the construction, performance, and operation of this system are given elsewhere.<sup>2,5</sup> The ultimate vacuum after bakeout of this system is usually  $3 \times 10^{-10}$  Torr; (although, in most recent work, it has been possible to reach a vacuum below  $10^{-10}$  Torr) with the main contaminants at this vacuum being  $\text{H}_2$ ,  $\text{H}_2\text{O}$ ,  $\text{CO}$ , and  $\text{CO}_2$ .

### B. UHV-microwave cavity

The heart of the experimental design is the X-band microwave cavity. The inner surface of the cavity supports the

surface to be studied, and therefore, it must be an integral part of the UHV system. Typical UHV-ESR cavities are discussed in detail elsewhere.<sup>2,5</sup> Our cavities are constructed from 0.020 in. thick titanium. These thin walls allow for field modulation (10, 25, and 100 kHz), while maintaining structural strength, and they allow for heat conductivity for temperature control. They are of a wide access cylindrical design and they operate in the TE<sub>011</sub> mode which provides a maximum in  $H_1$  field at the inner surface of the cavity. (The unwanted but degenerate TM<sub>111</sub> mode is eliminated in a standard manner.<sup>6</sup>)

UHV requires good pumping conductance between the cavity interior and the vacuum system. Conductance is poor with only the usual cavity "stack" design with a 1/2 in. diameter tube. We employ walls that are about 40% open and still maintain a  $Q_u$  of 8000 to 10 000.<sup>7</sup> Still, conductance is limited to 20  $\ell/\text{s}$  so there is some pressure difference between the cavity and the ion gauge, with the cavity usually slightly higher in pressure.

A static electric field in the cavity is found to be necessary when one wishes to suppress CREMSEE, and methods to accomplish this are described elsewhere.<sup>2,3,5</sup>

Finally, the temperature of the surface being studied is controlled by regulating the temperature of the cavity walls as noted above. This is done by passing cooled or heated nitrogen gas through the Teflon jacket outside the cavity walls; (this jacket also supports the coils for field modulation). Temperature is measured by a copper-constant thermocouple epoxied to the cavity wall. The temperature is read from a digital thermometer with 0.1  $^\circ\text{C}$  precision. We have performed experiments from  $-150$  to  $+150^\circ\text{C}$ .

The ESR sensitivity of the cavity compares well with the theoretical sensitivity. That is, we find a minimum detectable number of spins of  $5 \times 10^{11}$  spins per G linewidth. This is close to the theoretical value expected for our E-12 spectrometer with paramagnetic sample distributed uniformly over the 64  $\text{cm}^2$  inner surface of the cavity.<sup>2,5</sup> This gives an *average* sensitivity (see below) of nearly  $1 \times 10^{10}$  spins/G per  $\text{cm}^2$  surface area. (This may be compared to an estimated  $10^{15}$  atoms/ $\text{cm}^2$  on the metal surface.<sup>8</sup>)

ESR signal strength is calibrated and monitored with a  $\text{Cr}^{3+}$  doped ruby ESR intensity standard from the NBS. In all cases, digitalized first-derivative ESR signals are doubly integrated with appropriate base line subtraction. Also, due consideration was given for the different field-scan range and modulation amplitudes used. Since the ruby signal is significantly different from those of nitroxides, we tested the accuracy of the use of this standard by first comparing it with a sample of pure solid nitroxide (cf. Fig. 1). The use of the ruby standard led to an estimate of spins in the nitroxide sample that was within 10% of the actual number of spins in this reference sample, confirming the validity of using the ruby standard. The ruby standard was deemed the more appropriate in our UHV cavity, because (a) it could withstand the bakeout procedure; (b) it did not require a separate container; and (c) unlike a pure solid nitroxide sample, which has an exchange-narrowed ESR spectrum very similar to the ESR signal obtained from adsorbed layers of nitroxide, its signal will not interfere with observation of the latter.

For the actual SSERS experiments, the ruby was epoxied in place at a convenient spot on the inner wall of the cavity. Since the ESR sensitivity varies along the cavity wall due to variation in microwave magnetic field, we had first mapped out in detail the sensitivity as a function of position on the inner wall by varying the location of the ruby standard over the entire effective area. The above-noted signal sensitivity is based upon an integration over the whole surface, of the measured sensitivity as a function of location on the wall. Once the ruby standard was epoxied in place, the signal to noise (S/N) ratio was measured. Then this value was adjusted for the sensitivity at the location of the ruby, as compared to the average sensitivity. Further details of cavity sensitivity and spin concentration measurements are given elsewhere.<sup>5</sup> Because of the complexity of the SSERS experiments, and the necessity of making measurements during rapidly changing conditions, spin concentrations were measured only in a few cases. For the other cases, we relied on having the spectrometer performance not change very significantly from when a calibration was made. This was typically the case.

### C. Thin film deposition

The cylindrical cavity is ideal for our method of putting down a fresh and clean surface. A filament is brought into the cavity, and then a thin film of metal is deposited by evaporation at UHV. The filament is mounted on a bellows unit, which permits a linear travel of about 2 in. Our design keeps the filament lined up with the cavity axis. For silver a 5 mil diameter wire of 99.999% pure silver is wound on a molybdenum filament. For copper, a 5 mil diameter 99.999% pure copper wire is wound on a tungsten filament. The cavity is cooled to about 0 °C during the evaporation. This is in the range of temperature where the actual surface area should be greater than the geometrical area by no more than a factor of 1.3–1.4<sup>9</sup> because of grain coalescence.<sup>10</sup> These grains may be oriented with the (111) plane nearly parallel to the substrate.<sup>11</sup> For a large molecule such as a nitroxide, surface roughness should not have a great effect, because the roughness is on the order of molecular dimensions. The film deposited is 10 to 100 Å thick. The filament is retracted from the cavity by extending the bellows to permit ESR measurements.

Photo-CREMSEE<sup>4</sup> was used to measure the work function *in situ* in the microwave cavity. In this experiment UV light is directed onto the inner cavity surface, and the emitted photoelectrons are amplified and detected by the CREMSEE effect. We have made major improvements in the design of our apparatus since our earlier report.<sup>4</sup> These enabled us to (i) attain a large photon flux at the optimum surface in the ESR cavity, (ii) significantly improve light resolution; and (iii) allow for shorter  $\lambda$ . For a clean Ag surface at RT we find  $\phi = 4.25$  eV in good agreement with nonannealed Ag films.<sup>12</sup> Our previous result, for an air-oxidized Ag surface was  $\phi = 4.06$  eV, which is quite reasonable, especially in view of the fact that  $P_r$  for CREMSEE is decreased significantly by *air* oxidation.<sup>2,3,13</sup>

### D. General

Other experimental techniques used here are discussed below.

A Varian E-12 ESR spectrometer with a 12 in. magnet, is used in these experiments. The E-101 bridge is modified as prescribed by Varian for high  $Q$  cavity operation. The experiments described herein use either 10, 25, or 100 kHz modulation. The UHV-ESR system is wheeled into the magnet with the cavity centered in the magnetic field. The cavity is attached to the microwave bridge with a nonmagnetic flexible cable.

Production of a clean metal surface requires UHV. Routinely, this demands a bakeout of the system. The thin film is deposited at UHV and is studied immediately or left overnight at  $\sim 5 \times 10^{-10}$  Torr. No difference in results has been found.

Typically, all background measurements are taken at the working temperature before admitting any gas to the surface. The background mass spectrum may be recorded, the background ESR signal is recorded, and the threshold microwave power for CREMSEE ( $P_r$ ) is measured (see below).

Also, advance preparation is important because of the fast pace of dosage-dependent experiments. When all is prepared, the nitroxide or other gas is admitted while observing the ESR and  $P_r$ . Usually, this can be done at  $1 \times 10^{-8}$  Torr, so that even the effect of low dosages may be observed.

Measurements of  $g$  values reported here are made using a microwave frequency counter and an NMR gaussmeter. The precision of the frequency measurements is  $\pm 0.1$  MHz or  $\sim 1$  part in  $10^5$ , and the field measurements are  $\pm 0.1$  G from the gaussmeter. However, in practice the precision in magnetic field is about  $\pm 0.8$  G, because of large ESR linewidths, the variation in magnetic field over the sample distributed over the whole inner cavity surface, and the position of the gaussmeter probe away from the center of the field, due to the bulky UHV-ESR cavity plus cooling coils. Thus, the  $g$  values reported have a precision of  $\pm 0.005$  unless otherwise noted.

Pressures of nitroxides and other gases admitted are measured mostly by the ionization gauge. This gauge has not been calibrated for nitroxides. Varian lists sensitivity factors for many organic molecules. Based on that list we would crudely estimate that the pressure shown by the gauge is systematically too high for nitroxides, perhaps by a factor of 10. We do not correct for this factor in the results, which should to be regarded as "nominal values." This will not affect the relative values of pressure or dosage (defined as pressure multiplied by time of exposure) for any single nitroxide, but the relative values among the nitroxides might be affected somewhat. A particular value of the dosage,  $D_e$  is introduced in the next section. It is the nominal dosage at which an ESR signal first appears. It is obtained by extrapolating the ESR signal intensity as a function of dosage back to zero intensity.

The CREMSEE microwave power threshold,  $P_r$ ,<sup>2,3,5</sup> is measured as follows. The approximate resonance magnetic field is found well above  $P_r$  after first setting the field according to the known  $g$  value. The high field resonance is located

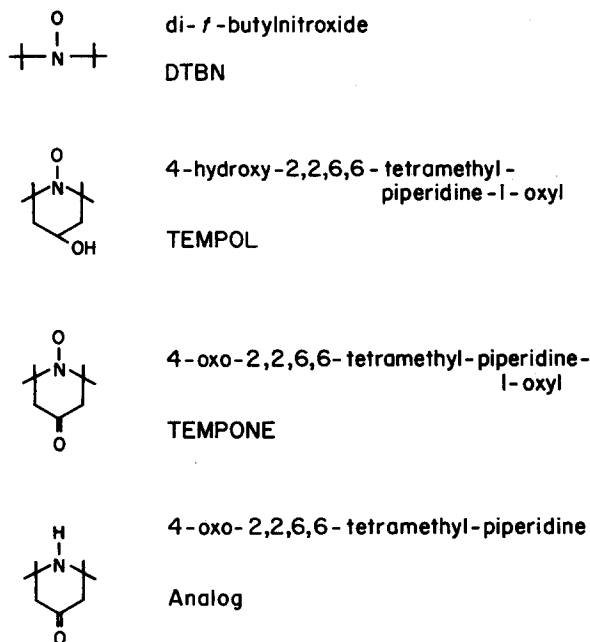


FIG. 1. Nitroxides used, their structures, descriptive names, and brief names.

and the exact position is established by adjusting the field setting for maximum detector signal while lowering the power. This consistently gives the correct position. Then the power is decreased carefully while observing the signal on the spectrometer oscilloscope. When the power passes below  $P_c$ , the CREMSEE signal disappears. This gives repeatable values for  $P_c$ . For this entire procedure, the modulation field is turned off, as no modulation is needed to observe the very strong and narrow signal.

In the present studies we have confirmed the previous observations,<sup>2,3</sup> viz. that a fresh clean metal surface gives a  $P_c$  about ten times that of the same metal surface with a high coverage of nitroxides; and also, that as molecules are desorbed from the surface by warming,  $P_c$  increases, approaching the value for the clean metal, which suggests nearly full desorption.<sup>14</sup>

Several nitroxides were used in these studies. These are shown in Fig. 1 and will be referred to henceforth by their brief names. DTBN and TEMPONE were obtained from Eastman Organic Chemicals, TEMPOL from Molecular Probes, and the perdeuterated Analog was synthesized in our labs by Eva Ignér. The nitroxides exhibit 100% paramagnetism in the bulk.<sup>15,16</sup> DTBN is a liquid and the others are solid at room temperature. All have an appreciable vapor pressure (0.2 to 2 Torr). Figure 2 shows the mass spectra of the nitroxides as well as the "clean" background. These mass spectra were taken with the quadrupole mass analyzer which is part of our UHV-ESR system.<sup>2,5</sup>

### III. RESULTS: SSERS

#### A. Clean Ag and Cu

Several nitroxides (shown in Fig. 1) were adsorbed and studied on clean Ag and Cu surfaces under a range of conditions. This is made convenient because they all have an ap-

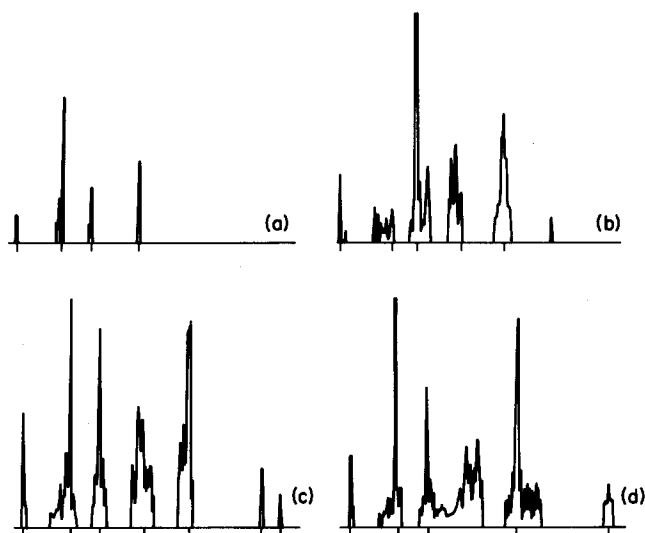


FIG. 2. Mass spectra of nitroxides. (a) Background, (b) DTBN, (c) TEMPONE, (d) Analog. Mass markers are at  $m/e = 2, 18, 28, 44, 56(b), 58(c,d), 83(c), 89(c,d)$ .

preciable vapor pressure (cf. Sec. II D). Most important, they are all 100% paramagnetic in the bulk (i.e., each molecule exhibits an unpaired spin), and they would be expected to remain paramagnetic in multilayers on the surface.

Freshly deposited silver gives no observable ESR signal at temperatures from RT to  $-150^\circ\text{C}$ . In no case does an ESR signal appear when the nitroxide is put down on the

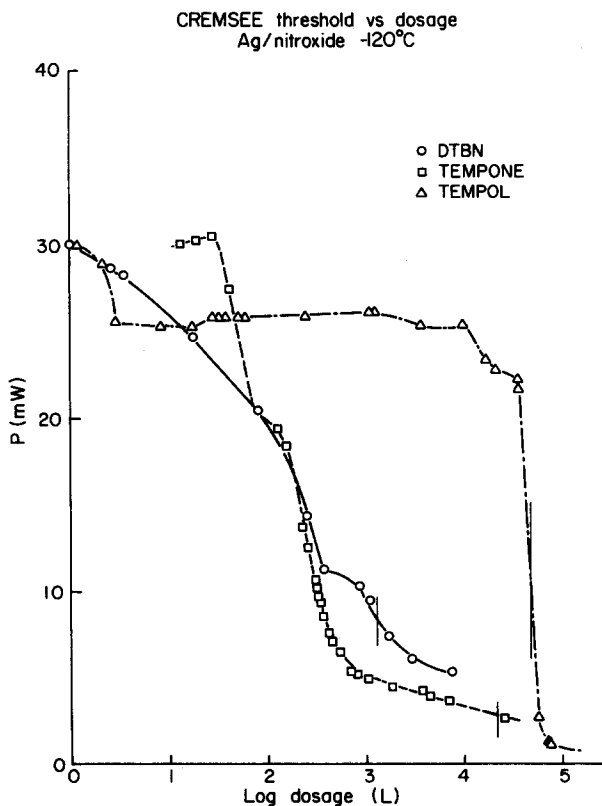


FIG. 3. CREMSEE  $P_c$  vs dosage in Langmuir ( $= 10^{-6}$  Torr s): Ag/DTBN, TEMPONE, and TEMPOL at  $-120^\circ\text{C}$ . Values are normalized so that the low (zero) dosage values coincide. Vertical marks indicate  $D_e$ .

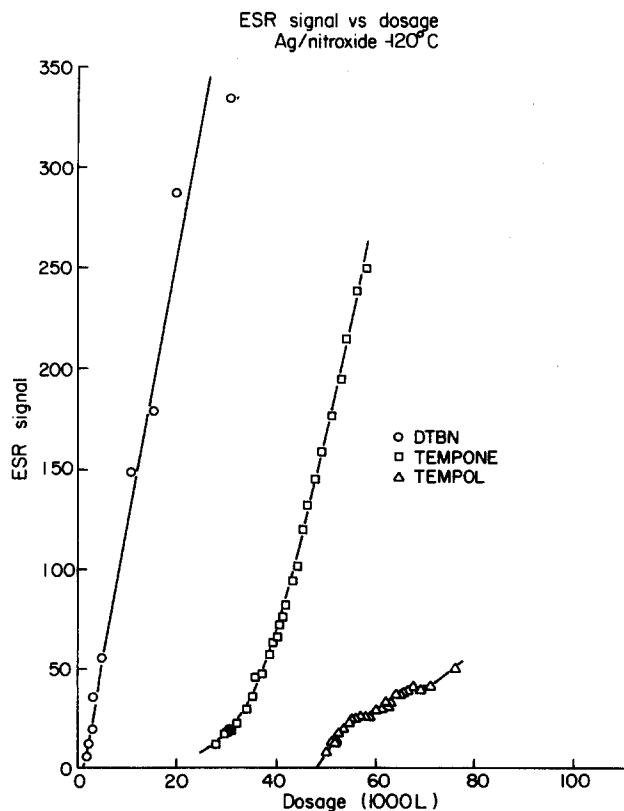


FIG. 4. ESR signal vs dosage (in Langmuir): Ag/DTBN, TEMPONE, and TEMPOL at  $-120^{\circ}\text{C}$ . Data are scaled such that nominal signal height of 100 corresponds to approximately  $2.1 \times 10^{15}$  spins per  $\text{cm}^2$  or 12 layers.

clean Ag or Cu surface until some threshold dosage,  $D_e$ , is reached. However, the CREMSEE  $P_i$  always drops by about an order of magnitude before this threshold is reached. From this we may conclude that the nitroxide is adsorbing on the metal and is bonding strongly enough to affect  $P_i$ . In Fig. 3 we show  $P_i$  vs dosage for adsorption of several nitroxides on clean Ag. These curves are quite different from the different nitroxides. At  $D_e$  (which is very different for each radical),

TABLE I. SSERS data for nitroxides.<sup>a</sup>

Nitroxide	$T_{\text{ads}}$ ( $^{\circ}\text{C}$ )	$D_e^b$ (kL)	$P_{i,e}/P_{i,0}$	$D_f^b$ (kL)	$P_{i,f}/P_{i,0}$
(A) Ag (and Au)					
DTBN	-150	2.5	0.12	30	0.07
DTBN	-116	1.3	0.26	31	$\sim 0.18$
TEMPONE	-125	22	0.09	58	$\sim 0.07$
TEMPONE	-55	112	0.33	149	$< 0.22$
TEMPOL	-120	47	0.20	76	0.04
Au/TEMPONE	-145	130	0.42	...	...
(B) Cu at $-120^{\circ}\text{C}$					
DTBN		3.0	0.074	46	0.045
TEMPONE		2.6	0.11	31.5	0.034

<sup>a</sup>  $T_{\text{ads}}$  = adsorption temp.  $P_{i,0} = P_i$  at 0 dosage.  $D_e$  = dosage when ESR first appears.  $P_{i,e} = P_i$  when ESR first appears.  $D_f$  = final dosage.  $P_{i,f} = P_i$  at final dosage.

<sup>b</sup> Based on uncorrected pressures. The actual  $D_e$  are more likely about an order of magnitude lower.

<sup>c</sup> Not measured.

the ESR signal appears and then continues to increase with further dosage as shown in Fig. 4 for the same set of experiments as in Fig. 3. The ESR signal that is observed is a single exchange-narrowed line with a derivative peak-to-peak linewidth of 11 G which is similar in each case. DTBN at  $-116^{\circ}\text{C}$  has the lowest nominal  $D_e$  of 1.3 kL ( $1 \text{ L} = 10^{-6}$  Torr s) with  $D_e$  significantly higher for the other cases [cf. Table I(A)]. At such temperatures for a large organic molecule, monolayer coverage is expected by 1–10 L (cf. Appendix A). This strongly suggests that several layers of physisorbed nitroxide are required before the ESR signal appears [even given that the actual pressures, hence the actual  $D_e$  are probably about an order of magnitude less than the nominal ones (cf. Sec. II D)]. This is most graphically illustrated in the curve of  $P_i$  vs dosage for TEMPOL in Fig. 3. There is an initial decrease in  $P_i$ , which we believe is due to the first, or chemisorbed, layer (here the nominal TEMPOL pressure is about  $10^{-8}$  Torr). There is no further change in  $P_i$  for several hours of dosage until the pressure was substantially increased to about  $10^{-5}$  Torr at which time a drop in  $P_i$  is observed. It may be possible that this is a case where, at the lower pressure, *net* physisorption may not be occurring onto the existing nitroxide surface (although its lower equilibrium vapor pressure at RT than that for DTBN is not supportive of this). In that case, one must raise the pressure above that for its condensation to obtain a net adsorption (cf. Appendix A). Alternatively, adsorption onto the first chemisorbed layer may be slow until a further layer is deposited. Nevertheless  $P_i$  must drop to 20% of its initial value in this case [cf. Table I(A)] before an ESR signal appears (i.e.,  $P_{i,e}/P_{i,0} = 0.20$ ), and the bulk of this drop occurs at the higher dosages.

The results for our experiments of nitroxides on Ag are summarized in Table I(A). One may observe that the effect of performing the experiment at a higher temperature is to increase  $P_{i,e}/P_{i,0}$ , while a significant increase in  $D_e$  is observed at higher temperatures (e.g., TEMPONE) where the sticking coefficient is expected to be reduced.

Thermal desorption studies of the nitroxide can provide information on the binding of different species on the surface. We show in Fig. 5 a thermal desorption study on TEMPONE in which the ESR signal and the pressure are monitored as temperature is increased from  $-125^{\circ}\text{C}$ , the temperature at which the initial adsorption occurs. One sees a definite maximum in ESR signal intensity<sup>17</sup> at  $-51^{\circ}\text{C}$ . ( $\equiv T_{em}$ ) after which there is a monotonic decrease in intensity leading to disappearance of the ESR signal at about  $-18^{\circ}\text{C}$  ( $\equiv T_{e2}$ ). When the experiment was repeated with a sample prepared at  $-55^{\circ}\text{C}$ , the desorption curve is nearly identical (above  $-55^{\circ}\text{C}$ ) to the curve obtained for  $-125^{\circ}\text{C}$ . The rise in pressure we observe at  $-95^{\circ}\text{C}$  ( $\equiv T_{d1}$ ) does not correspond to any significant change in ESR signal or in  $P_i$ . Nevertheless, by monitoring the mass analyzer during the desorption we find that the rise in pressure is due to the nitroxide and not to any background contaminant. The pressure peak at  $-20^{\circ}\text{C}$  ( $\equiv T_{d2}$ ) clearly corresponds to the species that gives rise to the ESR signal. Still  $P_i$  has not increased appreciably; this occurs slowly at a much higher temperature. The desorption of DTBN and

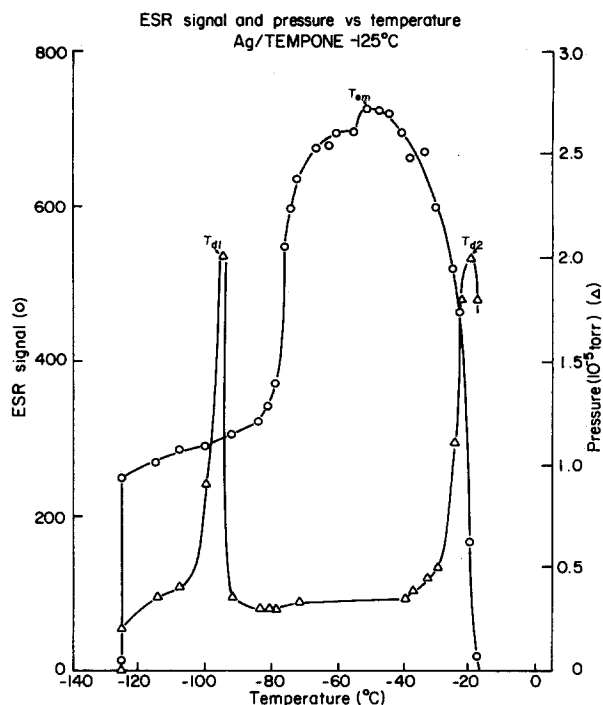


FIG. 5. ESR signal and pressure vs temperature: Ag/TEMPONE deposited at  $-125^{\circ}\text{C}$ . ESR signal height of 200 corresponds to approximately  $4.1 \times 10^{15}$  spins per  $\text{cm}^2$  or 25 layers.

TEMPOL is found to be qualitatively similar to that for TEMPONE. The characteristic features are summarized in Table II.

In a similar set of experiments for DTBN and TEMPONE on Cu the same general features were observed. In the case of Cu, however, the curves for  $P_i$  as a function of dosage are almost identical for these nitroxides as are the other parameters we measured for the adsorption process [cf. Table I(B)]. The two nitroxides desorb at different tem-

perature, but again the ESR signal intensity is found to first increase with temperature and then decrease.

The single run for Au using TEMPONE [cf. Table I(A)] yielded an unusually large value of  $D_e$  (130 kL) even though  $T = -145^{\circ}\text{C}$  was quite low. Also  $P_{i,e}/P_{i,0} = 0.42$  was rather high. These results are somewhat similar to those for Ag/TEMPONE at the higher  $T = -55^{\circ}\text{C}$  implying a reduced sticking coefficient as one might expect for Au. [We also note that unlike Ag or Cu, the fresh Au surface after deposition gave a broad (100 G) background ESR signal at  $g = 2.07$ .]

## B. Nitroxides on metals pretreated with oxygen

We originally found<sup>3</sup> that DTBN adsorbed on air-oxidized Cu (for periods of about a week) at RT gives a chemisorbed ESR signal with the conventional appearance of a dilute nitroxide ESR pattern as noted in Sec. II. We therefore undertook experiments to examine the sharp difference between results obtained with clean metal surfaces and air oxidized ones.

Experiments were performed on copper and silver pretreated with oxygen to try to form the clean insulator surface, or with wet oxygen to try to form hydroxyl groups on the surface. In every case, adsorption was performed at about  $-120^{\circ}\text{C}$ . Table II(A) shows the conditions of oxidation and the results. For air oxidation of copper,<sup>2</sup>  $P_i$  was found to decrease by about an order of magnitude, similar to the decrease in  $P_i$  preceding  $D_e$  for nitroxides on clean metals (cf. Table I). For cases 1–3 in Table III(A), the decrease in  $P_i$  with clean oxygen pretreatment is small. In case 1, of Ag/O<sub>2</sub>, the O<sub>2</sub> was present during deposition of the Ag thin film, in an attempt to perform reactive evaporation. This was not effective in reducing  $P_i$ . It is unclear whether large exposures ( $> 10^{12}$  L) of clean metal to pure oxygen will reduce  $P_i$ , even if the surface oxidizes. The secondary emission yield may not change significantly for the oxide. Silver is less reactive than copper, therefore less readily oxidized. This is seen in the

TABLE II. Summary of temperature data from combined ESR signal and thermal desorption studies.<sup>a</sup>

System	$T_{em}$	$T_{e1}$	$T_{e2}$	$T_d$
Ag/DTBN	-81	-80	-61	b
Ag/TEMPONE	-51		-18, -22 <sup>c</sup>	-95, -20
Ag/TEMPOL	-63	-53	-24	-106, -98
Cu/DTBN	-98		-57	-81, -65
Cu/TEMPONE	-53	-25	2	-4 <sup>d</sup>
Ag/O <sub>2</sub> /DTBN	-76		-55	b
Ag/O <sub>2</sub> + H <sub>2</sub> O/DTBN	-80		-58	b
Cu/O <sub>2</sub> /TEMPONE	-110, -73	-35	14	b
Cu/O <sub>2</sub> + H <sub>2</sub> O/TEMPONE	-90		-26	b
Cu/O <sub>2</sub> + H <sub>2</sub> O/DTBN	-94	-82	-70	b
Ag/1.4 kL Analog	-39	-20	19	b
Ag/8.3 kL Analog	-93, 17	-42	60	-84, 14, 60
Ag/14.5 kL Analog	-105, 25		61	-86, 25, 61

<sup>a</sup>  $T_{em}$  = temperature of maximum ESR signal in  $^{\circ}\text{C}$ .  $T_{e1}$  = temperature at which ESR signal starts to decrease prior to leveling off or increasing.  $T_{e2}$  = temperature at which ESR signal disappears.  $T_d$  = peaks in pressure.

<sup>b</sup> Not observed.

<sup>c</sup>  $-18^{\circ}\text{C}$  for case of TEMPONE initially deposited at  $-125^{\circ}\text{C}$ , and  $-22^{\circ}\text{C}$  for initial deposition at  $-55^{\circ}\text{C}$ .

<sup>d</sup> Additional small pressure peaks at  $-101$ ,  $-80$ , and  $55^{\circ}\text{C}$ .

TABLE III. SSERS data.<sup>a</sup>

System	$T_{ox}$ (°C)	$D_{ox}$ (L)	$P_{t,ox}/P_{t,c}$	$D_e^b$ (kL)	$P_{t,e}/P_{t,o}$	$D_f^b$ (kL)	$P_{t,f}/P_{t,o}$
(A) Nitroxides on oxides at -120 °C							
1. Ag/O <sub>2</sub> /DTBN	117	...	...	1.2	0.21	18.2	0.075
2. Ag/O <sub>2</sub> + H <sub>2</sub> O/DTBN	15	10 <sup>11</sup>	0.85	≤ 2.8	0.30	22	0.17
3. Cu/O <sub>2</sub> /TEMPONE	33	10 <sup>6</sup>	0.69	< 2	...	12.3	...
4. Cu/O <sub>2</sub> + H <sub>2</sub> O/TEMPONE	43	10 <sup>12</sup>	0.26	24.8	0.25	460	0.086
5. Cu/O <sub>2</sub> + H <sub>2</sub> O/DTBN	RT	10 <sup>14</sup>	0.18	3.3	0.31	8.0	0.32
	$D_A$ (kL)	$P_{t,A}/P_{t,c}$	$D_{e,T}^b$ (kL)	$P_{t,e}/P_{t,c}$	$D_f^b$ (kL)	$P_{t,f}/P_{t,c}$	
(B) TEMPONE on Ag pretreated with Analog							
	0	1.0	22	0.093	58	0.69	
	1.4	0.25	4.6	0.21	61	0.19	
	8.3	0.093	0	0.093	35	...	
	14.5	0.082	0	0.082	22	...	

<sup>a</sup>  $T_{ox}$  = temperature of oxidation.  $P_{t,c}$  =  $P_t$  of clean metal.  $D_A$  = dosage of Analog.  $P_{t,A}$  =  $P_t$  after depositing Analog.  $D_{ox}$  = dosage of oxygen.  $P_{t,ox}$  =  $P_t$  after oxygen. See Table I footnote a for further definitions.

<sup>b</sup> See Table I footnote b.

<sup>c</sup> Not measured.

greater drop in  $P_t$  for Cu/O<sub>2</sub> + H<sub>2</sub>O. Cases 4 and 5 are the only cases where  $P_t$  drops significantly.

We show in Fig. 6, the results with a copper surface that was kept under wet oxygen for one week, and which gave a large drop in  $P_t$  (case 5). Exposure to DTBN gave a further decrease in  $P_t$  as shown in Fig. 6(a). The ESR signal [Fig. 6(b)] appears at a dosage very near that for clean copper and DTBN. Also, the ESR signal observed is the same as that in the clean metal experiments. The ESR signal increases with temperature [Fig. 6(c)], as in other experiments, and decreases in two steps. (This increase in ESR signal could be accounted for by a continuation of adsorption.) The disappearance of the signal is at a somewhat low temperature, -70 °C.

### C. TEMPONE on silver pretreated with Analog

As we discuss below, we believe that the condensed layers of nitroxide insulate the subsequent layers from the metal surface. Also, the layers that are paramagnetic may interact with the earlier layers (close to the metal) by spin-exchange interactions. Therefore, we pretreated the surface with a molecule very similar to the nitroxide TEMPONE, except it is not paramagnetic. This molecule (Analog) differs from TEMPONE only by a substitution of H for O at the nitrogen (see Fig. 3). It should be very similar to TEMPONE in its adsorption on the silver surface if adsorption is not through the N-O group.

Adsorption of Analog was performed at -120 °C as for TEMPONE. Figure 7 shows  $P_t$  as a function of dosage. The three curves are almost identical and give an indication of the reproducibility. These curves differ from that for Ag/TEMPONE in requiring a larger dosage to cause  $P_t$  to drop. Progressively more Analog was put down on the surface in three runs. Table II(B) lists the dosages of Analog and other details for these experiments. After some dosage, the Analog

was pumped out and TEMPONE admitted. The appearance and growth of the ESR signal was followed, and the results are shown in Fig. 8. For pretreatment with 1.4 kL of Analog, the ESR signal appears at a much lower dosage than on clean silver [see Table III(B)]. The Analog is effective in covering the silver surface so that TEMPONE interacts less with the metal. After pretreating the silver surface with 8.3 kL of Analog, an ESR signal is observed. This is before any nitroxide is admitted. Thus, a paramagnetic species is formed from the Analog on the silver surface at a low temperature. The ESR signal increases with admission of TEMPONE. Another run was made with a higher dosage of Analog. In this run no signal was observed from Analog alone, but the signal does appear immediately with the admission of TEMPONE. [It is possible that, with the former run (8.3 kL), the surface warmed up momentarily during the last part of the adsorption of the Analog, permitting the oxidation of the nitrogen by a carbonyl of a neighboring molecule.]

The desorption data were also obtained. The curve for the 1.4 kL Analog run is similar to that for Ag/TEMPONE (Fig. 5) in that the ESR signal intensity increases considerably with temperature, but there is the additional feature, however, of a small increase before disappearance at a much higher temperature. The curves for 8.3 and 14.5 kL Analog are very similar to each other and rather different from those for lower dosages. The most notable feature here is the five-fold increase in ESR signal intensity to nearly the original maximum intensity with further warming after the initial large decrease. Figure 9 shows the ESR signal and pressure as a function of temperature. The first two small peaks in pressure correspond to the initial decrease in ESR signal. The next peak corresponds to the large second increase in ESR signal intensity, and the last rise in pressure corresponds to the disappearance of ESR signal. Note that the ESR signal does not disappear until the surface is warmed to 60 °C, well above room temperature, and the highest such temperature noted for any system.

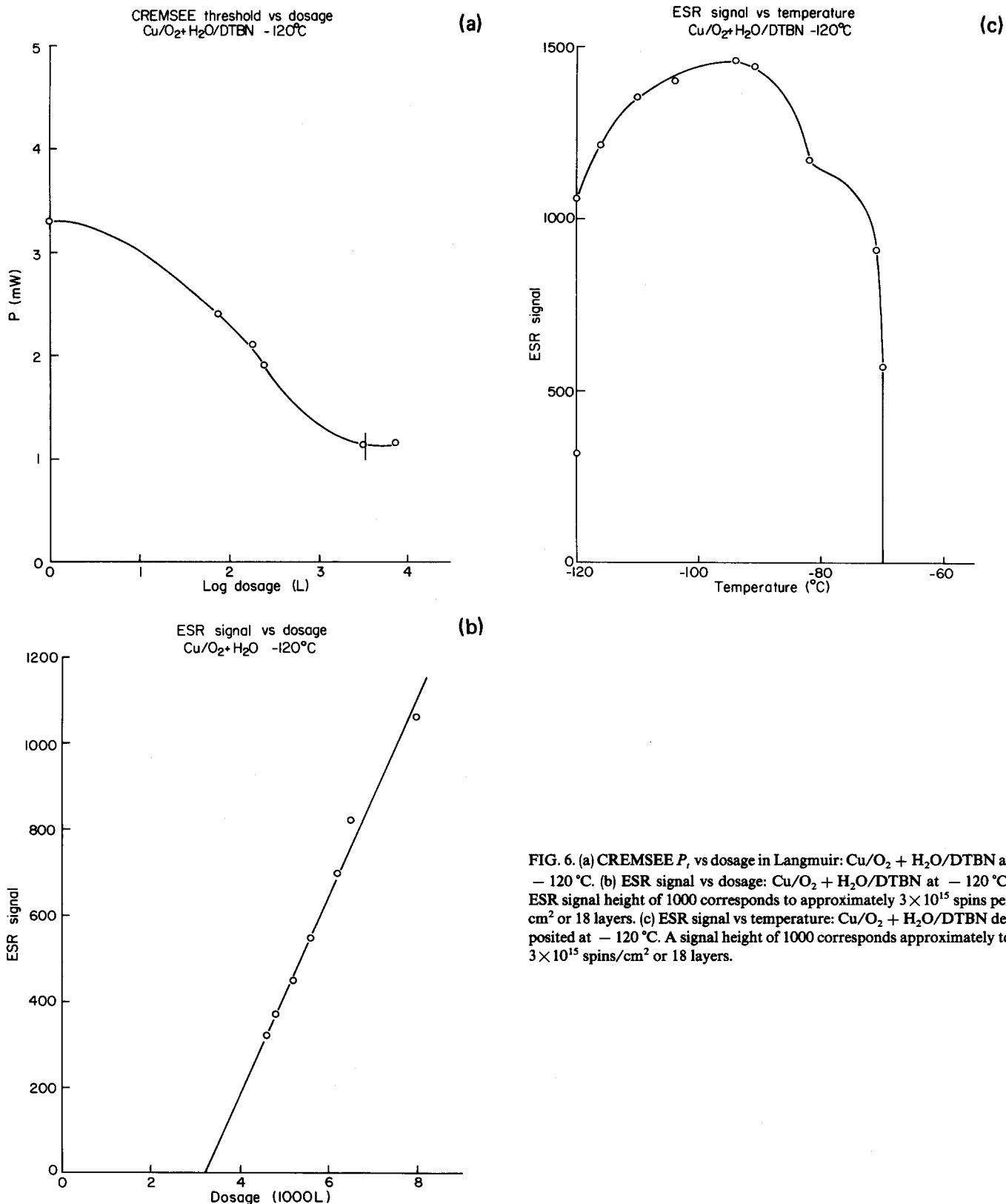


FIG. 6. (a) CREMSEE  $P$ , vs dosage in Langmuir:  $\text{Cu}/\text{O}_2 + \text{H}_2\text{O}/\text{DTBN}$  at  $-120^\circ\text{C}$ . (b) ESR signal vs dosage:  $\text{Cu}/\text{O}_2 + \text{H}_2\text{O}/\text{DTBN}$  at  $-120^\circ\text{C}$ . ESR signal height of 1000 corresponds to approximately  $3 \times 10^{15}$  spins per  $\text{cm}^2$  or 18 layers. (c) ESR signal vs temperature:  $\text{Cu}/\text{O}_2 + \text{H}_2\text{O}/\text{DTBN}$  deposited at  $-120^\circ\text{C}$ . A signal height of 1000 corresponds approximately to  $3 \times 10^{15}$  spins/ $\text{cm}^2$  or 18 layers.

#### D. ESR linewidths and $g$ values

The  $g$  value (cf. Sec. II D) measured for nitroxides on silver are very nearly those reported<sup>18</sup> for pure single crystals, within experimental error. The average value for DTBN is 2.0055 compared to 2.0059 for the single crystal,

for TEMPOL it is 2.0060 compared to 2.0062, and for TEM-PONE 2.0056 compared to 2.0068. Only for TEMPONE is there any significant difference, but this may still be accounted for by experimental error (cf. Sec. II D).

Linewidths of the ESR signal varied with coverage and temperature as shown in Fig. 10 for TEMPONE on silver



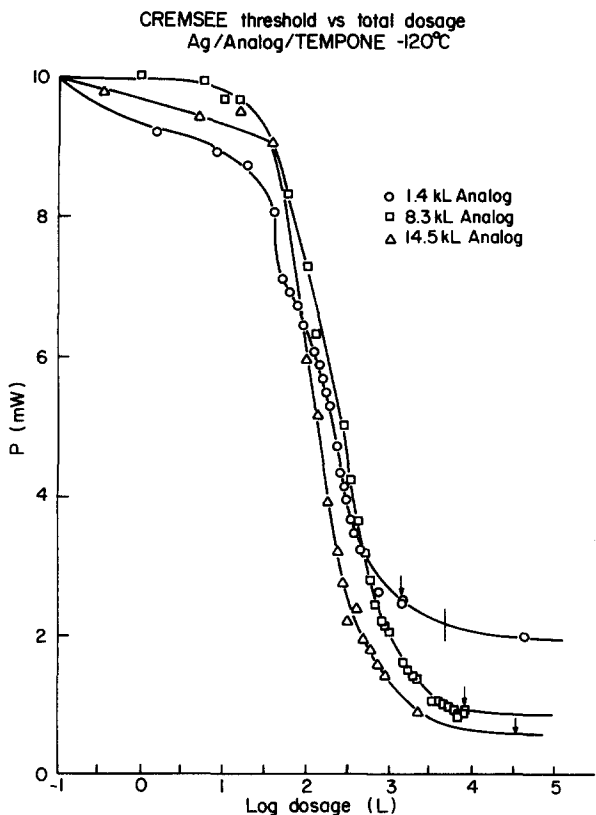


FIG. 7. CREMSEE  $P_t$  vs dosage: Ag/Analog/TEMPONE at  $-120^\circ\text{C}$ . Arrows show the break between Analog and TEMPONE adsorption.

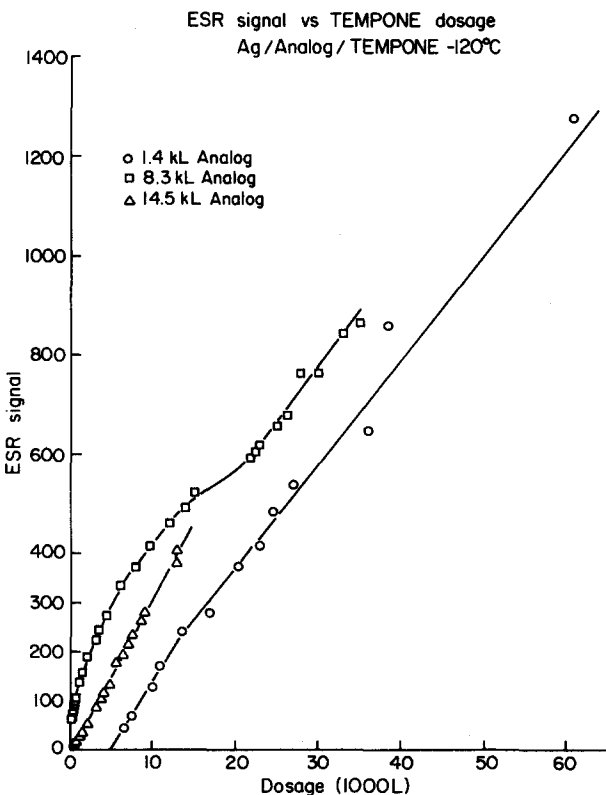


FIG. 8. ESR signal vs dosage: Ag/Analog/TEMPONE at  $-120^\circ\text{C}$ . ESR signal of 400 for the 1.4 kL curve corresponds to approximately  $3.8 \times 10^{15}$  spins per  $\text{cm}^2$  or 23 layers. For the other two curves, a height of 400 corresponds to approximately  $1.2 \times 10^{15}$  spins per  $\text{cm}^2$  or 7 layers.

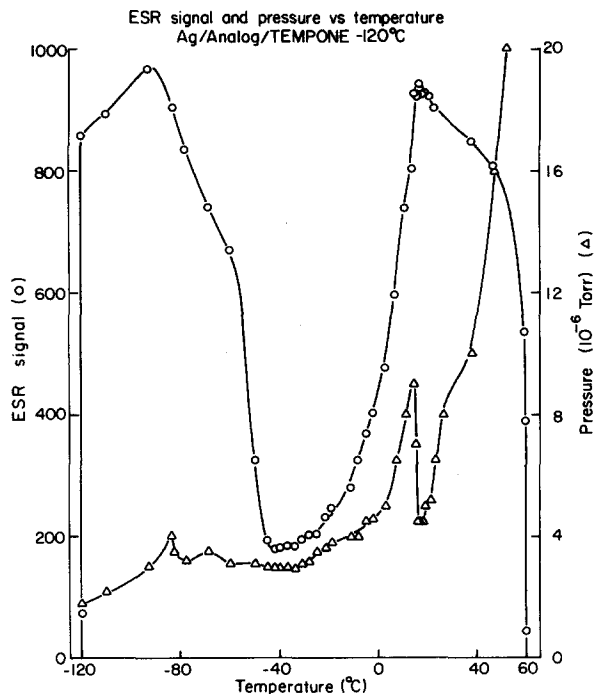


FIG. 9. ESR signal and pressure vs temperature: Ag/Analog/TEMPONE deposited at  $-120^\circ\text{C}$  for 8.3 kL Analog. ESR signal of 800 corresponds to approximately  $2.4 \times 10^{15}$  spins per  $\text{cm}^2$  or 14 layers.

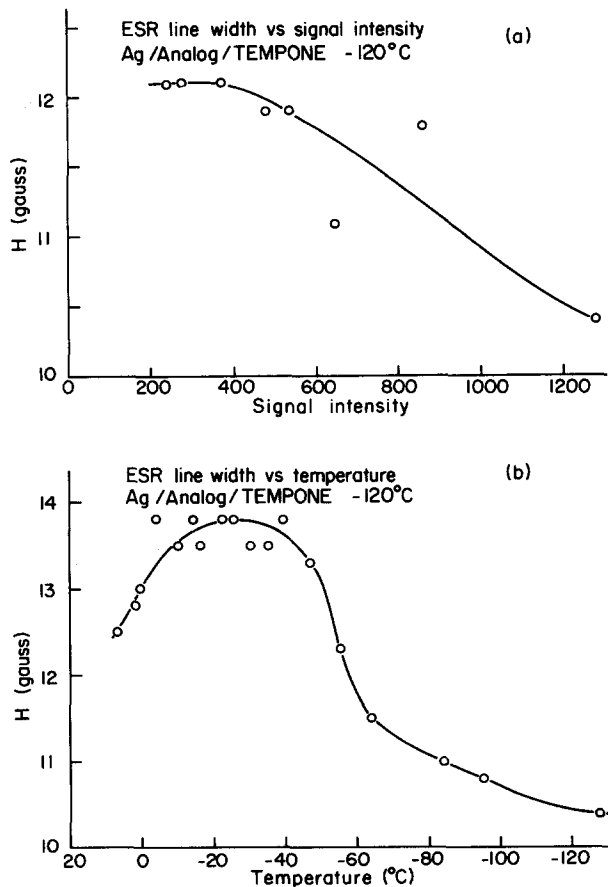


FIG. 10. ESR derivative linewidth vs ESR signal and temperature for 1.4 kL Analog pretreatment. Adsorption at  $-120^\circ\text{C}$ . (a) Line width vs ESR signal (cf. Fig. 8 caption for calibration); (b) linewidth vs temperature.

pretreated with 14 kL Analog. Linewidths were not regularly measured for the other cases because of the experimental difficulty associated with the rapidity of measurements taken as the temperature was varied. The ESR signal intensity reflects the extent of the coverage by the paramagnetic molecules. The line narrowing with coverage indicates an increase in net exchange interaction with coverage, or concentration of radicals, as expected. The change in linewidth with temperature is qualitatively very similar to that for solid DTBN.<sup>19</sup> In this case TEMPONE desorbs (19°) before it melts (36°),<sup>20</sup> and so should not exhibit liquid phase behavior. The maximum width reported here is very near that for solid DTBN but the low temperature value is somewhat higher than that for solid DTBN. This may be due to a greater distance between spins on the surface than in the bulk, or the low temperature limit may be reached more slowly with TEMPONE on the surface than bulk DTBN.

#### IV. DISCUSSION

In no case does an ESR signal appear when the nitroxide is first put down on the clean silver or copper or on the metal pretreated with oxygen (and water). Only after some minimum dosage,  $D_e$ , does an ESR signal become detectable. This dosage is greater than zero ( $\sim 10^3$ – $10^5$  L) [cf. Figs. 4 and 6(b)]. The drop in  $P_i$  for dosages up to  $D_e$  indicates that the surface is affected by dosages less than  $D_e$ . Our past and present work has shown that  $P_i$  decreases (increases) as the work function of the surface decreases (increases).<sup>13</sup> The work function decreases with adsorption of organic molecules on platinum<sup>21</sup> (e.g.,  $\Delta\phi = -1.6$  eV for 2, 6-dimethylpyridine), and thus the direction of change in  $P_i$  is consistent. It is assumed that the nitroxide is adsorbing on the metal or oxide surface and forming a surface dipole, thereby lowering  $P_i$ .

##### A. Sticking coefficients and SSERS coverage

Some estimate of the sticking coefficient  $\sigma$  would be useful. Based upon our observations, on simple models of adsorption of rare gases,<sup>17,18</sup> and utilizing the heat of vaporization of DTBN (which is 11 kcal/mol<sup>22</sup>), we would expect  $\sigma$  of order unity for the first layer on the metal. As the first layer begins to fill, physisorption begins to be important, for which  $\sigma$  should drop to some small but finite value. (Also, for conditions of our experiments we estimate that 1 L of dosage would give one monolayer coverage for  $\sigma \sim 1$ .) These matters are discussed in further detail in Appendix A.

In our experiments we can obtain data on  $\sigma$  for the physisorbed layers only when an ESR signal is observed. In particular, we can use our graphs of ESR signal vs dosage  $D$ . The ESR signal is first converted to absolute number of spins per  $\text{cm}^2$  of surface. This is transformed into the number of layers of detected spins,  $\theta$ , using the area occupied by one nitroxide molecule<sup>16</sup> (60 Å). Then  $\sigma = d\theta/dD$  (where we implicitly have used the estimate noted above and obtained in the Appendix that for  $\sigma = 1$  and  $D = 1$  L then  $\theta \approx 1$ ). Since we are ultimately interested in  $\sigma$  in order to determine  $\theta$ , for the layer(s) not observed by ESR, (i.e., the SSERS coverage), we might use  $\sigma_a \equiv d\theta/dD|_{D=D_e}$ , i.e., the initial slope at  $D_e$ .

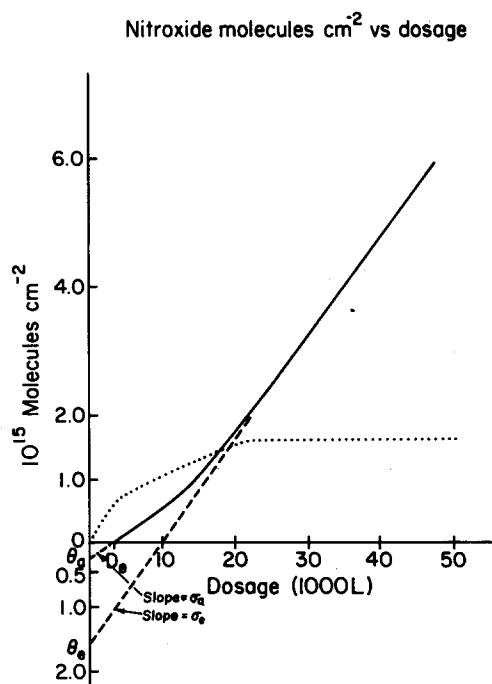


FIG. 11. Hypothetical case of nitroxide coverage vs dosage based on Cu/DTBN data. One layer is taken as  $1.6 \times 10^{14}$  molecules/ $\text{cm}^2$  (The  $\theta_a$  and  $\theta_e$  in the figure do not include the first strongly chemisorbed layer.)

This is shown graphically in Fig 11. These values are given in Table IV. It should be noted that in Table IV we have added one to the values obtained by the method of Fig. 11. This is to account for the first layer for which  $\sigma \approx 1$  (cf. above and Appendix A).

These results clearly suggest that the effect of the metal is to suppress ESR significantly (i.e., SSERS) beyond the first chemisorbed layer, i.e.,  $\theta_a > 1$ . Thus, it is likely that for  $D \sim D_e$  some nitroxide molecules are still experiencing SSERS, and  $\sigma_a$  is less than the true sticking coefficient. We have therefore made a second estimate of  $\sigma$ :  $\sigma_e = d\theta/dD|_{D \gg D_e}$ , i.e., we use the slope (of the usually straight line) of ESR signal vs  $D$  for  $D \gg D_e$ . Let us call the  $Y$  intercept of this line  $\theta_e$ . This is also shown graphically in Fig. 11. In most cases we find  $\sigma_e > \sigma_a$  as expected (cf. Table III). If we assume that either  $\sigma_a$  or  $\sigma_e$  is a reasonable estimate for  $\sigma$  during adsorption after the first layer even when no ESR signal appears, then we obtain an estimate of  $\theta$ ,  $\theta_a = \sigma_a D_e + 1$  and  $\theta_e \equiv \theta_e + 1$ . These values are likely to be estimates of the lower limit to  $\theta$ , because it is possible that not all molecules are ESR observable even for  $D \gg D_e$ . These estimates of  $\theta$  will not be affected by any calibration factor in the pressure measurement, since that cancels out in the above procedure. (Thus, as previously noted, the nominal  $D_e$  values in Tables I–IV are likely about an order of magnitude larger than the actual values, and consequently the nominal  $\sigma$ 's would be too small by the equivalent factor. The accuracy of  $\theta_a$  and  $\theta_e$  depends only on the calibration of the ESR signal intensity.) Thus the values of  $\theta_a$  and  $\theta_e$  in Table IV demonstrate that typically more than a monolayer coverage is required before an ESR signal is observed.

This conclusion is amplified by the observation of an

TABLE IV. Estimated parameters from SSERS data.<sup>a, b</sup>

System	$D_e^c$ (kL)	$\sigma_a^c$ ( $10^{-3}$ )	$\theta_a$	$\sigma_e^c$ ( $10^{-3}$ )	$\theta_e$	$R^d$
Ag/DTBN - 150 °C	2.5	1.1	3.8	1.2	6.2	0.12
Ag/DTBN - 116 °C	1.3	1.6	3.1	1.6	3.1	0.265
Ag/TEMPONE - 125 °C	22	0.23	6.1	1.3	48	0.093
Ag/TEMPONE - 55 °C	112	0.55	62	0.37	42	0.329
Ag/TEMPOL	47	0.42	21	0.15	(6.9)	0.204
Cu/DTBN	3.0	0.43	2.3	1.0	11	0.074
Cu/TEMPONE	2.6	1.5	4.9	1.9	8.8	0.110
Ag/O <sub>2</sub> /DTBN	1.2	0.90	2.1	2.3	5.4	0.206
Ag/O <sub>2</sub> + H <sub>2</sub> O/DTBN	2.8	~0	~1	1.0	3.1	0.298
Cu/O <sub>2</sub> /TEMPONE	1.0	5.8	6.8	4.7	7.0	... <sup>e</sup>
Cu/O <sub>2</sub> + H <sub>2</sub> O/TEMPONE	24.8	0.47	13	... <sup>f</sup>	... <sup>f</sup>	0.250
Cu/O <sub>2</sub> + H <sub>2</sub> O/DTBN	3.3	4.2	15	4.2	15	0.314
Ag/1.4 kL Analog/TEMPONE	4.7	1.6	8.5	1.2	(4.4)	0.211
Ag/8.0 kL Analog/TEMPONE	0	1.1	0	0.38	0	0.093
Ag/1.4 kL Analog/TEMPONE	0	0.41	0	0.72	0	0.080
Au/TEMPONE - 145 °C	130	... <sup>e</sup>	... <sup>e</sup>	... <sup>e</sup>	... <sup>e</sup>	0.42

<sup>a</sup> All adsorption performed at - 120 °C unless otherwise noted.

<sup>b</sup>  $\theta_a$ ,  $\theta_e$  are the numbers of adsorbed layers as described in the text.

<sup>c</sup> These are nominal values. Actual values for  $D_e$  are probably about an order of magnitude smaller while those of the sticking coefficients  $\sigma_a$  and  $\sigma_e$  about an order of magnitude larger (cf. the text).

<sup>d</sup>  $R = P_{t,e}/P_{t,0}$ . For the experiments with Analog we include the combined effects on  $P_t$  of deposition of Analog and of nitroxide [cf. Table III(B)].

<sup>e</sup> Not measured.

<sup>f</sup> Sharp decrease in slope after initial coverage, precluded a positive  $\theta_e$  by the method in the text.

increase in ESR signal as the temperature is raised in a number of our experiments, e.g., Figs. 5 and 9, as though there were a phase transition (cf. Sec. F) which leads to an increase in number of spins that give an ESR signal. These are cases where the increase is too great to be explained by any further deposition of nitroxide onto the surface.

We felt it to be of value to obtain independent confirmation of the number of layers deposited in these experiments. Desorption data can give a quantitative measure of this, and in at least one run our desorption data were of sufficient quality to permit such an estimate. This analysis<sup>23</sup> is supportive of the model of SSERS, i.e., more layers of nitroxide are deposited than are observed by ESR.

There is some possibility of error in  $\theta_a$  or  $\theta_e$  that could be true for a few cases (e.g., TEMPOL/Ag, cf. Fig. 3) where the early stages of dosage might have been at too low a pressure to have net adsorption (cf. Appendix A). In such cases, the effective  $D_e$  would be somewhat less than determined as in the illustration of Fig. 11. Just to estimate an upper bound for such an effect, we subtracted dosages at low pressure ( $\sim 10^{-8}$  Torr nominal) from the total dosages for those cases where such a possibility exists and recalculated  $\theta_a$  and  $\theta_e$ . In nearly all cases,  $\theta_a$  and  $\theta_e$  hardly decreased, and in all cases any decrease was well within other experimental uncertainties. This is simply because the bulk of the dosage always occurred at the higher pressures ( $\sim 10^{-5}$ – $10^{-6}$  Torr nominal), where, also, a concomitant decrease in  $P_t$  clearly indicated some form of adsorption. We suspect that, in future work, as the relationship between CREMSEE  $P_t$ , and the amount of surface coverage becomes clearer, that measurement of  $P_t$  would itself be a useful index of coverage.

## B. CREMSEE $P_t$ and SSERS

We are inclined to regard the layers giving rise to SSERS as performing the role of insulating the metal surface, so that further layers can give an ESR signal as noted above. To the extent that  $P_t$  is a measure of surface chemisorption and/or to the buildup of a total surface dipole, we might expect that  $P_{t,e}$  (i.e., the threshold value of  $P_t$  when an ESR just appears) would be indicative of this insulating effect. One hypothesis would then be that the relative threshold value,  $R \equiv P_{t,e}/P_{t,0}$  might be a constant. This would be consistent with the simple model that  $R$  is a measure of the shielding from the metal surface, and the shielding necessary for the ESR signal to appear is the same in all cases. The results in Table IV yield an average  $R = 0.19 \pm 0.09$ . In view of the many experimental difficulties and uncertainties, this may be a reasonable result in favor of this hypothesis. But, some variation with system (e.g., the metal and its pretreatment) might be expected, so we may try to relate to  $R$  to the coverage, i.e., to  $\theta_e$ . We have found that most of the relevant data in Table IV (not counting pretreatment with Analog, or wet H<sub>2</sub>O, or the higher  $T$ , - 55 °C run) could be fit to the expression:  $(R^{-1} - 1) = m\theta_e$  with  $m = 1.02 \pm 0.11$  (and a correlation coefficient of 0.81). Such a correlation simply states that the decrease in  $P_t$  at ESR threshold is directly proportional to the coverage at ESR threshold, which would seem quite reasonable.

We also see from Table IV that the apparent sticking coefficients,  $\sigma_e$ , are rather similar in most cases, i.e., they are mostly in the range of about  $(1-2) \times 10^{-3} \text{ L}^{-1}$  nominal even though  $\theta_e$  appears to vary considerably. The case of Ag/

TEMPONE at  $-55\text{ }^\circ\text{C}$  is lower, most likely because of the higher temperature. There is some indication that pretreatment of the surface by wet  $\text{O}_2$  or by Analog can reduce  $\sigma_e$  while pretreatment by dry  $\text{O}_2$  might increase it somewhat. The anomalously low value of  $\sigma_e$  for Ag/TEMPOL is not understood. It appears inconsistent with the higher desorption temperatures  $T_{e2}$  for TEMPONE and TEMPOL as compared to DTBN (cf. Table II), suggesting that the strength of adsorption is greater for the first two nitroxides, as one would expect if their "tail" functional groups are involved significantly in the adsorption (cf. below). Perhaps it is indicative of an important steric (or geometric) factor<sup>24</sup> in the adsorption mechanism for TEMPOL, e.g., the hydroxyl group might have to be favorably aligned relative to the surface. Clearly, more accurate experiments are required to study such variations in  $\sigma_e$ . In particular, we remind the reader it was not conveniently possible to regularly monitor the ESR sensitivity, so possible variations from one experiment to another can be expected to introduce some uncertainty in relative values of  $\theta_e$  (or  $\theta_a$ ) and  $\sigma_e$  (or  $\sigma_a$ ).

### C. Analog

The important role of shielding of those molecules further away from the surface by those that are near the surface, appears to be confirmed by our experiments with the diamagnetic-Analog molecule. A moderate predosage with Analog does significantly reduce the  $D_e$  and  $\theta_e$  required to observe an ESR signal, while a large predosage provides sufficient shielding that an ESR signal was observed from lowest dosages of TEMPONE.

Also TEMPONE on Analog-pretreated Ag showed the most unusual temperature behavior (cf. Fig. 9). There is an initial large decrease in ESR signal, which is clearly not due to desorption. Instead it is most likely due to a transition from paramagnetic to diamagnetic of a large portion of the adsorbed nitroxide molecules. This transition reverses at a higher temperature to give full paramagnetism once again. The actual desorption which occurs at  $60\text{ }^\circ\text{C}$  is much higher than any other system studied, suggesting a stronger attraction to the surface for the mixture of analog and TEMPONE. We have no explanation for this.

### D. Pretreated surfaces

Results for  $D_e$ ,  $\sigma_e$ ,  $\theta_e$ , and  $R$  on Ag pretreated with  $\text{O}_2$  or  $\text{O}_2/\text{H}_2\text{O}$  differed little from the results on clean Ag. This may be explained by the relative inertness of Ag to oxygen adsorption, incorporation, and oxidation.<sup>25</sup> The sticking coefficient for  $\text{O}_2$  above 0.1 monolayer coverage is no more than  $10^{-5}$  with 1 Torr  $\text{O}_2$  required for monolayer coverage.<sup>25(a)</sup> Incorporation of  $\text{O}_2$  into the bulk is very slow,<sup>25(b)</sup> therefore little oxidation is expected. As a result, most metal atom sites for DTBN adsorption are still available.  $\text{O}_2$  pretreatment has a greater effect on Cu. Adsorption of dry  $\text{O}_2$  on Cu slightly reduces  $D_e$  and  $\theta_e$  and possibly slightly raises  $\sigma_e$ . Adsorption of wet oxygen prior to adsorption of nitroxides increases  $D_e$ , slightly increases  $\theta_e$ , and reduces  $\sigma_e$ , while the increase in  $R$  is significant. Copper is more reactive than Ag, demonstrating adsorption and incorporation of  $\text{O}_2$ .<sup>26-28</sup> For higher dosages of  $\text{O}_2$ , the Cu surface is found to restructure

such that Cu atoms are always exposed to the impinging gas.<sup>26,29</sup> Thus Cu atoms are probably available at the surface to interact with the nitroxide.

These results for nitroxides adsorbed on  $\text{O}_2$  or  $\text{O}_2/\text{H}_2\text{O}$  pretreated Cu at  $-120\text{ }^\circ\text{C}$  are very different from those we previously obtained for DTBN adsorbed on air oxidized Cu at room temperature<sup>3</sup> and noted above. The major difference is that after evacuation of the physisorbed layer(s), a typical hyperfine structure for nitroxides was seen previously,<sup>3</sup> but not in our current experiments. Another difference is that the ESR signal of DTBN or TEMPONE in the present experiment was found to disappear below  $2\text{ }^\circ\text{C}$ , whereas the adsorption on air oxidized copper was performed at RT and the signal persisted to at least  $58\text{ }^\circ\text{C}$ . Either there is some other component from air (e.g., sulfides,  $\text{N}_2$ ,  $\text{CO}_2$ ) providing an (insulating) site that has high binding energy for the nitroxide, or else at RT, activated adsorption at sites unavailable at  $-120\text{ }^\circ\text{C}$  becomes possible.

### E. Other studies

There are some reports of loss of paramagnetism of nitroxides with adsorption on surfaces under medium vacuum or by wet methods but not by UHV. No ESR signal is observed with the initial adsorption of DTBN on the surface of  $\text{Al}_2\text{O}_3$ , although a signal is subsequently observed for higher coverage.<sup>22</sup> A similar result is seen on a zeolite<sup>22</sup> and on  $\text{Al}_2\text{O}_3/\text{SiO}_2$ ,<sup>22,30,31</sup> where no ESR signal is observed for the initial coverage and subsequent coverage gives approximately 50% paramagnetism. In all of these cases, the loss of paramagnetism is attributed to decomposition<sup>22,31</sup> or to protonation.<sup>32</sup> This effect could be explained by interaction of the unpaired electron with the surface as explained below. In one case<sup>32</sup> for DTBN adsorbed on Pt/ $\text{Al}_2\text{O}_3$  or Pt/ $\text{SiO}_2$ , no ESR signal was observed for the nitroxide adsorbed on the platinum, whereas the nitroxide adsorbed on surface hydroxyls did give an ESR signal. This is the most similar to our results, but not identical, as DTBN may adsorb preferentially on the hydroxyls.<sup>32</sup> Hydrogenation of the nitroxide on Pt/ $\text{SiO}_2$  is possible even at  $-70\text{ }^\circ\text{C}$ , causing the ESR signal to immediately disappear.<sup>32,33</sup>

### F. Model

Our tentative model for the phenomenon of SSERS based on the above observations is as follows. The first or chemisorbed layer is interacting strongly by exchange (and other) forces with the surface conduction band of the metal. On the basis of rough order-of-magnitude estimates based on the "electronic" Korringa effect<sup>34,35</sup> this coupling should lead to a  $T_2 \sim T_1 \sim 10^{-11}$  s or a huge linewidth of 5.7 kG, which would render the ESR signal unobservable. Subsequent nitroxide layers interact with the preceding layers by a weak exchange interaction  $J \sim 10^{11} - 10^{12}$  s<sup>19,36</sup> (but see below). We would expect a progressively weaker transmission of the effects of the surface metal conduction band to each subsequent layer until it is ultimately no longer important to the spin properties of the layer. (There could also be the possibility of some direct exchange to the surface conduction band as well as this indirect mechanism if the interaction is

sufficiently long range. Preliminary calculations indicate that a direct mechanism might be necessary to yield SSERS.)

The fact that an increase in temperature can first increase the ESR signal in some cases [i.e., number of observable spins; cf. Figs. 5, and 9 and Table III(B)] might be correlated with Fig. 10 which shows a rise in ESR linewidth with temperature. This latter observation of linewidth variation with temperature is similar to what has been observed in pure solid samples of DTBN, where it was studied at different Zeeman frequencies.<sup>19</sup> Kreilick's<sup>19</sup> interpretation for bulk samples was in terms of a change in  $J$  and in average intermolecular separation between nitroxides taking place as a function of temperature. Such thermal effects as changes in  $J$  could very well modulate the number of surface layers which experience SSERS if this tentative model is valid. (The effective exchange interaction may also be modified by the coverage, cf. Fig. 10.) Further work would be needed to establish this potentially important correlation.

If there is residual interaction with the surface conduction band in the observed ESR signal, then this might show up as a small shift in the  $g$  value from that of the pure nitroxide, and that shift might be expected to be smaller with further coverage. We have measured  $g$  values only after significant coverage, and we observe some hint of a slight decrease in  $g$  values. However, in our previous work<sup>3</sup> on DTBN, the incipient  $g$  value just above  $D_c$  was found to be 2.0039, or a more significant decrease. According to our model, the  $g$  shift would be the electron-spin equivalent of the usual nuclear Knight shift.<sup>35</sup> Again further work on very accurate  $g$  shifts with coverage would be helpful.

Ultimately, experiments at 4 K and below would be very helpful, since at these low temperatures the conduction band ESR signal is narrow enough to be seen.<sup>35,37</sup> and if this model of SSERS is correct, then by analogy to the study of dilute alloys in Cu,<sup>35,37,38</sup> the surface nitroxides could also be visible in the ESR and show interesting effects due to their coupling to the metals. One may then deduce from such effects important properties of the dynamic electronic interactions between surface paramagnets and the surface conduction band.

Up until now, our discussion has been implicitly based upon the assumption that the physisorbed layers of nitroxide would behave similarly to bulk solid nitroxide. The temperature-dependent anomalies reported above might well imply that this is not necessarily true. In fact, one should consider the well-known phenomenon of wetting. That is, the initial physisorbed layers must adapt to the constraints of the attractive substrate, thereby forming film with characteristics that can be different from that of the solid bulk material.<sup>39</sup> Complete, or type 1 wetting, implies an infinite film thickness before there is coexistence with the bulk; while incomplete, or type 2 wetting implies some critical thickness of the film before condensation of the bulk; and in type 3 or "non-wetting" there is only bulk condensation.<sup>40</sup> If there is a relatively large substrate attraction, then the first few adsorbed layers can be compressed by these substrate forces to densities greater than the bulk. This would lead to a structural mismatch of the film with that of the bulk crystal, so the latter would begin to form once the attractive effects of the

substrate are no longer felt by the later adsorbed layers (i.e., type 2 wetting).<sup>41</sup>

If we introduce this consideration into our model for SSERS, then we might suppose that higher densities of the surface "film" would imply a much greater exchange coupling between the nitroxide molecules than experienced in the bulk. This could (a) enhance the suggested indirect exchange coupling of the subsequent layers to the metal surface (and maybe even a direct coupling) and (b) if  $J$  becomes of the order of  $kT$  in the "film," and is antiferromagnetic<sup>15</sup> the paramagnetism could be suppressed. Both possibilities would help explain SSERS. Furthermore, some of the temperature-dependent anomalies could be explained as due either to lattice expansion within the film with change in temperature and/or a phase transition to a lower density "wetting phase,"<sup>42</sup> both of which could modify  $J$  and hence the observed ESR signal strength. (There is also the possibility of phase transitions that depend upon the coverage<sup>42</sup> as desorption takes place at higher  $T$ .) Thus, considerations of a "wetting film," and its distinct structural and paramagnetic properties, could very well be important in understanding SSERS.

## V. CONCLUSIONS

It has been possible to study the interaction of stable paramagnetic species with clean noble metal surfaces. By means of UHV-ESR, CREMSEE, and thermal desorption experiments, we have observed the phenomenon of SSERS, whereby the stable nitroxide radicals appear to lose their paramagnetism upon adsorption onto the metal surface. We find this to be true in *all* cases for the several nitroxides and noble metals studied in the present work. The present experiments, including those with a similar but diamagnetic species, show that this loss of paramagnetism persists even beyond the first chemisorbed layer, suggesting a model of "insulating layers" of adsorbed molecules which must be put down on the surface before ESR signals appear. Furthermore, there is the indication of transformations in the properties of the adsorbed layers as a function of temperature (and possibly coverage) which affect SSERS.

## ACKNOWLEDGMENTS

We wish to thank Professor Robert Merrill, Professor Robert Silsbee, and Dr. Mark Nilges for many very helpful and stimulating discussions.

## APPENDIX A: Sticking Coefficients

Some basic understanding of the sticking coefficient is useful in analyzing our results. At low temperatures such as those used in this work, chemisorption typically proceeds through a physically adsorbed precursor.<sup>18</sup> The population of the precursor  $[P]$  is assumed to remain constant, thus,

$$\frac{d[P]}{dt} = k_p C - (k'_p [P] + k_a [P]) \simeq 0,$$

so that

$$[P] = \frac{k_p C}{k'_p + k_a},$$

where  $k_p$  is the rate of physical adsorption,  $C$  is the concentration of the vapor (proportional to pressure),  $k_p'$  is the rate of desorption from the precursor, and  $k_a$  the rate of transfer into the chemisorbed state  $A$ . Then the rate of chemisorption becomes

$$\frac{d[A]}{dt} = k_a [P] \simeq \frac{k_p C}{k_p'/k_a + 1}$$

Assuming  $k_a$  depends on coverage according to the simple form  $k_a = k'(1 - \theta)$  and substituting yields

$$\frac{d[A]}{dt} = \frac{k_p k' C}{k_p'(1 - \theta) + k'}$$

with an initial rate ( $\theta = 0$ ) given by

$$\left(\frac{d[A]}{dt}\right)_0 = \frac{k_p k' C}{k_p' + k'}$$

A model developed for rare gases<sup>43,44</sup> may be adapted to the present case to estimate the initial rate. The model assumes adsorption in a square well potential of depth  $D$ . Trapping (sticking) occurs when the thermal energy of the molecule can be accommodated by the collision with the surface. Accommodation is determined by the relative masses of the surface (metal) atoms and the colliding (nitroxide) molecule. Since the well depth was related, in this model, to the heats of vaporization  $\Delta H_v$  for the rare gases, we estimate the well depth for DTBN by comparison of heats of vaporization for rare gases to that of DTBN. The  $\Delta H_v$  for DTBN is 11 kcal mol<sup>-1</sup><sup>22</sup> at 25 °C. This is greater than that for krypton<sup>45</sup> or xenon<sup>46</sup> the rare gases with the largest  $\Delta H_v$ . Thus we estimate an initial sticking coefficient of one, as expected for such a large molecule. (A larger value of  $D$  would, of course, not change this result.)

The rate of chemisorption diminishes with coverage to zero at a full monolayer according to the above model. The way in which the rate depends on coverage is determined by the ratio  $k_p'/k'$ , but the average sticking coefficient is no less than 0.5 for the first monolayer according to this model. As the first layer fills, physisorption begins to be important. Therefore, the sticking coefficient should not go to zero but rather to some small value. This value is, of course, the important one for multilayer adsorption.

The vapor pressure of the nitroxide at the adsorption temperature indicates at what partial pressure significant condensation onto the surface by the nitroxide is expected to occur. Using the Clausius-Clapeyron equation, assuming a constant heat of vaporization over the temperature range 20 to -120 °C, the vapor pressure is

$$\ln P = -\frac{\Delta H_v}{R} \frac{1}{T} + \text{const.}$$

The const is determined from the known vapor pressure for DTBN of 1.4 Torr at 25 °C.<sup>32</sup> This gives a vapor pressure at -120 °C of  $3 \times 10^{-8}$  Torr where condensation begins. When the variation in  $\Delta H_v$  with  $T$  is taken into account, we estimate a lower value of  $4 \times 10^{-9}$  Torr at -120 °C.<sup>47</sup>

Finally the sticking coefficient must be carefully defined for the range of conditions of these experiments. The net rate of adsorption,  $W$ , is a function of exposure, temperature, and

coverage, i.e.,  $W = \sigma Z = \sigma'(\theta, T)Z - k_d f(\theta, T)$ , where  $\sigma$  is the net sticking coefficient (defined by the first equality),  $Z$  the collision rate (defined below),  $\sigma'$  the actual sticking coefficient which is a function only of coverage and temperature,  $k_d$  the desorption rate constant, and  $f$  a function of coverage and temperature. The actual sticking coefficient is not a function of pressure. It is defined as the probability that a molecule striking the surface will stick. The net sticking coefficient is more nearly the quantity measured in these experiments. At equilibrium at a given  $T$ , there is no net adsorption, i.e.,  $\sigma'Z_e = k_d f$ , where  $Z_e$  is the collision rate at the equilibrium pressure. For our experiments, adsorption was usually conducted at -120 °C and significantly above  $10^{-9}$  Torr (even allowing for a possible factor of 10 difference between the nominal and actual measured nitroxide pressures). Thus, the desorption rate, which should be equal to the adsorption rate at  $\sim 4 \times 10^{-9}$  Torr according to our above estimate, would be small compared to the adsorption rate at, say,  $3 \times 10^{-6}$  Torr which is a typical pressure utilized. Under these conditions  $W = \sigma Z \approx \sigma'Z$  so the two sticking coefficients are equal. This also means that dosage should be a valid measure of coverage at constant temperature. In a few cases such as that of TEMPOL/Ag, the experimental evidence (cf. Fig. 3 and Sec. III) suggests that net adsorption might not be occurring at lower pressures ( $\sim 10^{-8}$  Torr nominal) but requires higher dosage rates. However, this appears inconsistent with the significantly lower equilibrium vapor pressure of TEMPOL at RT compared to DTBN.

We now consider  $Z$  the rate of molecular collisions with the surface. It is given by elementary kinetic theory as<sup>44</sup>

$$Z = 3.5 \times 10^{22} P(TM)^{-1/2} \text{ molecules cm}^{-2} \text{ s}^{-1},$$

where  $P$  is in Torr,  $T$  in degrees K, and  $M$  is the gram molecular weight. For these experiments, the inlet temperature for the gas is about 296 K. The molecular masses range from 144 to 172, giving only a 9% range in  $Z$ . For a pressure of  $1 \times 10^{-6}$  Torr,  $Z = 1.6 \times 10^{14}$  molecules cm<sup>-2</sup> s<sup>-1</sup>. Thus, in 1 s, i.e., 1 L, there are  $1.6 \times 10^{14}$  collisions per cm<sup>2</sup> corresponding to one collision per 60 Å<sup>2</sup>, which is just the area occupied by one nitroxide molecule.<sup>16</sup> One Langmuir of dosage therefore, would give about one monolayer coverage if every molecule colliding with the surface were to stick (i.e.,  $\sigma = 1$ ). The simplicity of this result is, of course, accidental; it is due to the range of temperatures and molecular masses utilized.

<sup>1</sup>M. Nilges, M. Shiotani, C. T. Yu, G. Barkley, Y. Kera, and J. H. Freed, *J. Chem. Phys.* **73**, 588 (1980).

<sup>2</sup>M. Nilges, G. Barkley, M. Shiotani, and J. H. Freed, *J. Chim. Phys.* **78**, 909 (1981).

<sup>3</sup>M. Nilges and J. H. Freed, *Chem. Phys. Lett.* **82**, 203 (1981).

<sup>4</sup>M. Nilges and J. H. Freed, *Chem. Phys. Lett.* **85**, 499 (1982).

<sup>5</sup>G. Barkley, Ph.D. thesis, Cornell University, 1983.

<sup>6</sup>I. G. Wilson C. W. Schramm, and J. P. Kinzer, *Bell Syst. Tech. J.* **25**, 408 (1946).

<sup>7</sup>M. C. Thompson, Jr., F. E. Freethey, and D. M. Waters, *IRE Trans. Microwave Theory Technol.* **MTT-7**, 388 (1959).

<sup>8</sup>D. Haneman, in *Characterization of Solid Surfaces*, edited by P. F. Kane and G. B. Larrabee (Plenum, New York, 1974), Chap. 14, p. 337.

<sup>9</sup>T. Rhodin (private communication).

<sup>10</sup>J. V. Sanders, in *Chemisorption and Reactions on Metal Films*, edited by J. R. Anderson (Academic, New York, 1971), Chap. 1, p. 1.

- <sup>11</sup>J. G. Allpress and J. V. Sanders, *J. Catal.* **3**, 528 (1964).
- <sup>12</sup>(a) A. W. Dweydari and C. H. B. Mee, *Phys. Status Solidi A* **17**, 247 (1973); (b) **27**, 223 (1976).
- <sup>13</sup>We were able to further correlate our method of measurement of  $\phi$  with that of other workers, and also to demonstrate a correlation with the quantity  $P_i$  measured by CREMSEE and measurements of  $\Delta\phi$ . We studied slow  $O_2$  adsorption on Ag which had previously been studied by more conventional means. We obtained the expected increase in  $\Delta\phi$  with  $O_2$  dosage, and the magnitude of  $\Delta\phi$  is of the same order as previously measured for single-crystal surfaces [cf. Refs. 12(a) and 25(b)]. In another run we compared  $\Delta\phi$  and  $R = P_{i,e}/P_{i,o}$  vs  $O_2$  dosage. We find that they show similar trends, i.e., they both increase (at a similar rate) with  $O_2$  dosage, but while  $P_i$  changed by 10% (after a  $4 \times 10^4$  L dosage)  $\Delta\phi$  had changed by only 2%. We feel this demonstrates the correlation between  $P_i$  changes and  $\Delta\phi$  for adsorption studies, and again points out the great sensitivity of  $P_i$ .
- <sup>14</sup>In previous work we have proposed that changes in  $P_i$  should be relative to changes in  $E_p$ , the incident electron energy necessary for  $\delta = 1$  (i.e., a secondary electron emission yield of unity) (Ref. 3). A proper theory for the effects of surface adsorption on CREMSEE should consider how  $\delta$  varies with the full distribution of energies ( $Ep$ ) of the incident electron and how such a curve is modified by the adsorption. Data of  $\delta$  vs  $Ep$  are given in O. Hachenberg and W. Braner [in *Advances in Electronics and Electron Physics*, edited by L. Morton (Academic, New York, 1959), Vol. XI, pp. 413–499]. While  $Ep_1$  for Au and Ag are comparable, we found that CREMSEE appears easier to start for Au (i.e., a lower value of  $P_i$ ). This would be consistent with its significantly larger values of  $\delta$  for  $Ep > Ep_1$  (Hachenberg and Braner). A more dramatic indication of the role of  $\delta$  in the CREMSEE phenomenon comes from a study of freshly prepared Al surfaces. It was impossible to generate CREMSEE in the case of Al! This correlates with the fact that for Al,  $\delta < 0.95$  for all values of  $Ep$ . After only a small exposure of the Al surface to  $O_2$  (at 90 °C), CREMSEE was easily produced. This is to be expected, since  $Al_2O_3$  has a  $\delta_{max}$  of 1.5–9 (cf. Hachenberg and Braner). Thus the requirement that  $\delta > 1$  for some values of incident electron energies in order to cause CREMSEE, seems to be confirmed by this observation.
- <sup>15</sup>M. S. Davis, C. Mao, and R. W. Kreilick, *Mol. Phys.* **29**, 665 (1975); D. Ondercin, T. Sandreczki, and R. W. Kreilick, *J. Magn. Reson.* **34**, 151 (1979).
- <sup>16</sup>(a) *Spin Labeling Theory and Application*, edited by L. J. Berliner (Academic, New York, 1976); (b) J. Lajzerowicz-Bonneteau, *ibid.* Chap. 6, p. 239.
- <sup>17</sup>At constant  $T$ , the signal would be expected to increase somewhat due to further adsorption. But the increase observed is much greater than that expected from adsorption, especially considering the smaller sticking coefficient predicted for higher temperatures.
- <sup>18</sup>*Magnetic Resonance in Colloid and Surface Sciences*, ACS Symp. Ser. 35, edited by H. A. Resing and C. G. Wade (American Chemical Society, Washington, D.C., 1976).
- <sup>19</sup>C. R. Mao and R. W. Kreilick, *Chem. Phys. Lett.* **34**, 447 (1975).
- <sup>20</sup>L. R. Mahoney, G. D. Mendenthal, and K. U. Ingold, *J. Am. Chem. Soc.* **95**, 8610 (1973).
- <sup>21</sup>M. Salmeron and G. A. Somorjai, *J. Phys. Chem.* **85**, 3835 (1981). J. L. Gland and G. A. Somorjai, *Adv. Colloid Interface Sci.* **5**, 205 (1976).
- <sup>22</sup>G. P. Lozos and B. M. Hoffman, *J. Phys. Chem.* **78**, 2110 (1974).
- <sup>23</sup>In the case of DTBN on Cu, an estimated 120 layers of nitroxide are desorbed. Approximately 40 paramagnetic layers were observed by ESR before the desorption took place, while 11 diamagnetic layers were estimated to be present, for a total of about 51 layers. Various measurement errors could account for the factor of 2 difference. However, this result is supportive of the result based on ESR measurement: A substantial number of layers of nitroxide are deposited, and the apparent sticking coefficient is of the correct order of magnitude.
- <sup>24</sup>On  $SiO_2$  and  $Al_2O_3$ , TEMPONE and TEMPOL appear to adsorb flatly through both active groups, N–O and C≡O or N–O and OH with the C≡O or OH forming a stronger bond with the surface than the N–O [E. V. Lunina, A. K. Selivanovskii, V. B. Golubev, and B. V. Strakhov, *Vestn. Mosk. Univ., Ser. 2: Khim.* **20**, 131 (1979)]. On gold prepared under atmospheric conditions (not clean), TEMPOL and a nitroxide with an alkane tail similar to DTBN stick through the OH or C–H tail, not the N–O [R. B. Clarkson and S. McClellan, *J. Catal.* **62**, 551 (1980)]. Thus, different sticking coefficients for the various nitroxides would be reasonable.
- <sup>25</sup>(a) P. G. Hall and D. A. King, *Surf. Sci.* **36**, 810 (1973); (b) H. A. Engelhardt and D. Menzel, *ibid.* **57**, 591 (1976).
- <sup>26</sup>T. A. Delchar, *Surf. Sci.* **27**, 11 (1971).
- <sup>27</sup>C. Benndorf, B. Egert, G. Keller, H. Seidel, and F. Thieme, *J. Vac. Sci. Technol.* **15**, 1806 (1978).
- <sup>28</sup>C. Benndorf, E. Egert, G. Keller, H. Seidel, and F. Thieme, *J. Phys. Chem. Solids* **40**, 87 (1979).
- <sup>29</sup>P. Hoffman, R. Unwin, W. Wyrobisch, and A. M. Bradshaw, *Surf. Sci.* **72**, 635 (1978).
- <sup>30</sup>A. K. Selivanovskii, V. B. Golubev, E. B. Lunina, and B. V. Strakhov, *Russ. J. Phys. Chem.* **52**, 1617 (1978).
- <sup>31</sup>G. P. Lozos and B. M. Hoffman, *J. Phys. Chem.* **78**, 200 (1974).
- <sup>32</sup>M. M. Mestdagh, G. P. Lozos, and R. L. Burwill, Jr., *J. Phys. Chem.* **79**, 1944 (1975).
- <sup>33</sup>Hydrogen is one component of the residual gas in our UHV system and could perhaps react with the nitroxide as suggested in Ref. 30. Suppose the partial pressure of  $H_2$  is  $5 \times 10^{-10}$  Torr (see Fig. 2) and the sticking coefficient is the same as for the nitroxides. This would give at most one  $H_2$  sticking per 20 nitroxide molecules, assuming the nitroxide pressure is  $10^{-8}$  Torr. (It is almost always higher.) With 100% efficiency of reaction, this would give only a 10% reduction in free radicals. At higher pressures of nitroxide typically used, the effect of residual hydrogen is nil since  $H_2$  partial pressure hardly changes. Some other effect must account for the lack of ESR signal.
- <sup>34</sup>J. Koringa, *Physica* **16**, 601 (1950).
- <sup>35</sup>J. Owen, M. Brown, W. D. Knight, and C. Kittel, *Phys. Rev.* **102**, 1501 (1956).
- <sup>36</sup>M. P. Eastman, R. G. Kooser, M. R. Das, and J. H. Freed, *J. Chem. Phys.* **51**, 2690 (1969).
- <sup>37</sup>A. Raizman, J. T. Suss, D. N. Seidman, D. Shaltiel, and V. Zevin, *Phys. Rev. Lett.* **46**, 141 (1981).
- <sup>38</sup>P. Monod and S. Schultz, *Phys. Rev.* **173**, 645 (1968).
- <sup>39</sup>R. Pandit, M. Schick, and M. Wortis, *Phys. Rev. B* **26**, 5112 (1982), and reference therein.
- <sup>40</sup>(a) J. L. Seguin, J. Suzanne, M. Beinfait, J. G. Dash, and J. A. Venables, *Phys. Rev. Lett.* **51**, 122 (1983); (b) J. Krim, J. G. Dash, and J. Suzanne, *ibid.* **52**, 640 (1984).
- <sup>41</sup>R. J. Muirhead, J. G. Dash, and J. Krim, *Phys. Rev.* **329**, 5074 (1984).
- <sup>42</sup>(a) R. J. Birgeneau, M. Sutton, and S. G. J. Machrie, *Phys. Rev. Lett.* **51**, 407 (1983); S. Satija, L. Passell, J. Eckert, W. Ellenson, and H. Patterson, *ibid.* **51**, 411 (1983).
- <sup>43</sup>R. P. Merrill (private communication).
- <sup>44</sup>W. H. Weinberg and R. P. Merrill, *J. Vac. Sci. Technol.* **8**, 718 (1971); R. P. Merrill (private communication).
- <sup>45</sup>W. B. Street and L. A. K. Staveley, *J. Chem. Phys.* **55**, 2495 (1973).
- <sup>46</sup>W. B. Street, L. S. Sagan, and L. A. K. Staveley, *J. Chem. Thermodyn.* **5**, 633 (1973).
- <sup>47</sup>Taking account of the variation in  $\Delta H_v$  with  $T$  requires estimating  $V = \int \Delta c_p dT$ , where  $V$  is the change in  $\Delta H_v$  and  $\Delta c_p$  the difference in heat capacities of the liquid and the gas. If we ignore the very small temperature dependence in  $\Delta c_p$ , then we may estimate  $V$  by analogy to similar liquids to be about  $-15 \text{ cal mol}^{-1} \text{ K}^{-1}$  [cf. W. J. Moore, *Physical Chemistry*, 4th ed. (Prentice-Hall, Princeton, 1972), p. 132f]. Thus,  $\Delta H_v \approx -15(T - 298) + 111\,000 \text{ cal mol}^{-1}$ . Then the Clausius–Clapeyron equation is  $\ln p \approx 1 \int [-15(T - 298) + 11\,000]/T^2 dT$  yielding the above result.